

DOI: 10.63527/1607-8829-2025-2-5-16

Yu.V. Lutsiuk¹ (<https://orcid.org/0000-0003-1776-6734>),
V.M. Kramar^{1,2} (<https://orcid.org/0000-0002-3185-4338>),
I.A. Konstantynovych^{1,2} (<https://orcid.org/0000-0001-6254-6904>),
O.M. Voitsekhivska¹ (<https://orcid.org/0000-0003-2118-231X>)

¹Yuriy Fedkovych Chernivtsi National University,

2 Kotsiubynsky str., Chernivtsi, 58012, Ukraine;

²Institute of Thermoelectricity of the NAS and MES
of Ukraine, 1 Nauky str., Chernivtsi, 58029, Ukraine

Corresponding author: V.M. Kramar, e-mail: v.kramar@chnu.edu.ua

Effect of Acoustic Phonons on Thermoelectric Properties of Lead Iodide Nanofilms

The effect of spatial confinement on the propagation velocity of acoustic phonons in planar quasi-2D nanostructures (nanofilms) based on the layered semiconductor 2H-PbI₂, thermal conductivity coefficient and thermoelectric figure of merit is investigated within the approximation of elastic continuum using the elasticity theory. It is shown that the biggest influence on the thermal conductivity of lead iodide nanofilms is exerted by acoustic phonons, which belong to the dilatational vibrations of the crystal lattice atoms. The predominant mechanism of relaxation of all types of confined acoustic phonons in a nanofilm at a moderate concentration of impurities is the phonon-phonon (Umklapp) interaction. Its efficiency depends on the nanofilm thickness and temperature. The velocities of phonons propagation also depend on these parameters. These features lead to a rapid decrease of thermal conductivity at smaller nanofilm thickness and bigger temperature, contributing to increasing thermodynamic figure of merit of the nanostructure. Estimation of the thermodynamic figure of merit for ultrathin (several layers of 2H-PbI₂) films bring to the conclusion that they are suitable for the fabrication of thermoelectric devices, which can operate at room and higher temperatures.

Keywords: nanostructure, phonon, spectrum of frequencies and group velocities, thermal conductivity, thermoelectric figure of merit, thermoelectric materials, lead iodide.

Introduction

The development of nanomaterials synthesis technologies for the needs of modern electronics is accompanied by active research of the wide range of their physical properties.

Citation: Yu.V. Lutsiuk, V.M. Kramar, I.A. Konstantynovych, O.M. Voitsekhivska (2025). Effect of Acoustic Phonons on Thermoelectric Properties of Lead Iodide Nanofilms. *Journal of Thermoelectricity*, (2), 5–16. <https://doi.org/10.63527/1607-8829-2025-2-5-16>

This is explained by the perspectives of the low-dimensional, in particular quasi-two-dimensional, structures in production of various electronic devices, including thermoelectric ones, operating in the range of room and higher temperatures [1–5].

Layered semiconductors are considered as the most suitable for germanium, tin and lead iodide nanostructures [6, 7]. The latter, PbI_2 , is characterized by a rather high stability, unlike, for example, GeI_2 [8, 9]. In addition, some new technologies for obtaining nanostructures based on it have been developed recently. In particular, flat crystalline structures of hexagonal symmetry with a thickness of several layers of lead iodide are obtained by vapour deposition [6, 10], growth from colloidal solutions [11] or mechanical exfoliation from bulk 2H- PbI_2 crystals [12]. Thus, it becomes particularly attractive for the fabrication of various electronic devices: planar light sources [6] and solar cells [13], high-temperature X - and γ -ray detectors [14, 15], as well as for the other thermoelectric needs [16].

As for the search of materials, which would be suitable for the efficient thermoelectric devices, much attention is drawn to those with high electrical conductivity, big thermal electromotive force and low thermal conductivity [1]. Such combination of properties ensures the achievement of sufficiently high magnitudes of the thermoelectric figure of merit of the material

$$zT = \frac{\sigma S^2 T}{\kappa}, \quad (1)$$

here σ is the specific electrical conductivity, S and κ are the Seebeck and thermal conductivity coefficients, respectively. The effect on the electrical and thermal conductivity of semiconductor low-dimensional structures is possible due to the changes in their phonon spectra, since thermal activation of impurity conductivity and heat transfer inside them is carried out mainly by acoustic phonons. The spectra of frequencies and group velocities of such structures are significantly rearranged when their sizes change. In particular, decreasing nanofilm thickness leads to decreasing group velocities of acoustic phonons. As a result, it changes the thermal conductivity of nanofilm. Thus, the appropriate selection of the structure sizes can solve the problems of phonon engineering [17, 18].

Over the past two decades, a considerable number of results of experimental and theoretical studies of the phonon spectrum and thermoelectric properties of bulk (3D), thin and monolayer (2D) PbI_2 crystal structures have been published [19–23]. However, these results for the structures with different sizes were obtained by different methods and, therefore, cannot be extended to the determining of their thermoelectric properties at arbitrary thickness.

Guided by the concept of phonon engineering and the idea of studying the transformation of the phonon spectrum within an unified approach, we calculated the spectra of frequencies and group velocities of acoustic phonons for 2H- PbI_2 nanofilms [24] and analyzed the changes in their average propagation velocities at various nanofilm thickness and temperature [25].

It was shown that the dispersion curves of the energies and group velocities of all modes of confined acoustic phonons change nonlinearly if both the phonon wave vector length and the nanofilm thickness varies. In particular, at decreasing thickness, the propagation velocities of

phonons, depending on their polarization and temperature, can be reduced by a factor of times for shear-polarized phonons and by a factor of tens for SA- and AS-polarized phonons [26]. This result confirms the assumption that it is possible to tune the physical properties, including thermoelectric ones, by appropriate selection of 2H-PbI₂ nanofilm thickness.

In this paper, the effect of changing nanofilm thickness for 2H-PbI₂-type structure on the thermal conductivity coefficient and, accordingly, the thermoelectric figure of merit is evaluated.

1. Problem statement and model for the research

In quasi-two-dimensional structures the propagation of acoustic phonons and, thus, the heat is usually described within the framework of the elastic continuum model [26, 27]. It allows to present the lattice component κ_L of the thermal conductivity coefficient $\kappa = \kappa_e + \kappa_L$ in the form

$$\kappa_L = \frac{1}{4\pi k_B T^2 d} \sum_{\alpha, n} \int_0^{q_{\max}} [\hbar \omega_n^\alpha(q) v_n^\alpha(q)]^2 \tau_c(\omega_n^\alpha) \frac{\exp\left(\frac{\hbar \omega_n^\alpha(q)}{k_B T}\right)}{\left(\exp\left(\frac{\hbar \omega_n^\alpha(q)}{k_B T}\right) - 1\right)^2} q dq, \quad (2)$$

which is obtained taking into account the density of states of the phonon system [17]. Here, k_B – is the Boltzmann constant, d is the nanofilm thickness, α , $\omega_n^\alpha(q)$ and $v_n^\alpha(q)$ are the polarization, frequency, and group velocity of the phonon from the n -th mode of the spectrum, respectively; q is the quasi-momentum and $\tau_c(\omega_n^\alpha)$ is the complete phonon relaxation time. To determine the latter, the Debye-Callaway model is usually used. It takes into account all possible relaxation mechanisms: phonon-phonon scattering, phonon scattering on free surfaces, impurities, and dislocations [18, 28].

The electron component of the thermal conductivity coefficient κ_e , according to the Wiedemann-Franz-Lorentz law, is expressed within the electrical conductivity σ by the relationship

$$\kappa_e = L\sigma T, \quad (3)$$

where L is the Lorentz constant [16].

According to formula (2), in order to calculate κ_L , it is necessary to have an explicit form of the dispersion laws for the frequencies and group velocities. The frequencies $\omega_n^\alpha(q)$ can be obtained within the framework of the elastic continuum model as a solutions of a secular problem based on the equations of vibrations in an elastic medium. They contain the characteristics of both the vibrations (components of the displacement vector) and the medium (its density ρ and elastic constants c_{ij}). The equations of motion of all possible types of acoustic vibrations, characteristic to hexagonal symmetry nanostructures (shear, flexural and dilatational vibrations) together with the analysis of solutions obtained by numerical methods for the example of AlN/GaN/AlN structure are presented in [27].

In order to obtain analytical dependences, we have been proposed a method for solving a similar problem for nanofilm-type structures using the Fourier expansion of the amplitudes of the displacement vector components for the elastic vibrations of the atoms in crystal lattice [29]. It made possible to obtain the energies $\hbar\omega_n^\alpha(q)$ and group velocities of each of the acoustic vibration modes as functions of the wave vector q . In the case of a problem with boundary conditions, which correspond to the free nanofilm surfaces, they are written as

$$\omega_n^{sh}(q) = \sqrt{\frac{c_{66}q^2 + c_{44}(n\pi/d)^2}{\rho}}, \quad (4)$$

$$v_n^{sh}(q) = \frac{c_{66}q}{\sqrt{\rho_0(c_{66}q^2 + (\frac{\pi n}{d})^2 c_{44})}} \quad (5)$$

for the shear vibration mode and

$$\omega_n^{SA/AS}(q) = \sqrt{\frac{F_{1n}(q) \pm \sqrt{F_{2n}(q)}}{2\rho}}, \quad (6)$$

$$v_n^{SA/AS}(q) = \{[(c_{11} + c_{44})\sqrt{F_{2n}(q)} \pm (\frac{n\pi}{d})^2 [2(c_{13} + c_{44})^2 - (c_{11} - c_{44})(c_{33} - c_{44})]]q \pm \pm(c_{11} - c_{44})^2 q^3\} [2\rho F_{2n}(q)(F_{1n}(q) \pm \sqrt{F_{2n}(q)})]^{-1/2} \quad (7)$$

for the modes of dilatational (SA) and flexural (AS) phonons. Here, n is the number of mode (quantum number of the vibrational state), d is the nanofilm thickness (parameter, which should be specified).

$$F_{1n}(q) = (c_{11} + c_{44})q^2 + (n\pi/d)^2(c_{33} + c_{44}) \quad (8)$$

and

$$F_{2n}(q) = (c_{11} - c_{44})^2 q^4 + 2(n\pi/d)^2 [2(c_{33} + c_{44})^2 - (c_{11} - c_{44})(c_{33} - c_{44})] q^2 + (n\pi/d)^4 (c_{33} - c_{44})^2 \quad (9)$$

are the auxiliary functions [29]. If $n = 0$, formulae (2–5) determine the velocity dispersion laws for TA_2 -, LA - and TA_1 -modes of normal vibrations in a bulk (3D) crystal, respectively.

The details of the calculation of the lattice thermal conductivity coefficient using dependences (4–7) and the estimation of the thermoelectric figure of merit for 2H-PbI₂-type nanofilms of hexagonal symmetry are presented further.

2. Calculation methodology and results

A characteristic feature of the layered semiconductor structure PbI₂ is that nearly flat surfaces without dangling bonds are formed in the direction of layer growth [30]. Due to the

low density of surface defects, the surfaces of quasi-two-dimensional PbI_2 structures are almost perfectly smooth [11]. Owing to the high carrier mobility, they exhibit high electrical conductivity, which is caused by the activation of impurity conduction by acoustic phonons [16]. Therefore, we neglect phonon scattering at surfaces and consider only phonon-phonon scattering and scattering at ionized impurities.

Within the Debye-Callaway model, the both phonon-phonon scattering mechanisms: normal (N) scattering and Umklapp (U) processes are taken into account. Their relaxation times are given by the formulas presented in [28]. In the notation adopted here, they can be written as

$$\frac{1}{\tau_N(\omega_n^{\text{SA}})} = \frac{k_B^3 \gamma_{\text{SA}}^2 V_0}{\hbar^2 M (v^{\text{SA}})^5} (\omega_n^{\text{SA}})^2 T^3, \quad \frac{1}{\tau_N(\omega_n^{\text{AS/sh}})} = \frac{k_B^4 \gamma_{\text{AS/sh}}^2 V_0}{\hbar^3 M (v^{\text{AS/sh}})^5} \omega_n^{\text{AS/sh}} T^4, \quad (10)$$

$$\frac{1}{\tau_U(\omega_n^\alpha)} = \frac{\hbar \gamma_\alpha^2 V_0}{M \Theta_\alpha (v^\alpha)^2} (\omega_n^\alpha)^2 T \exp\left(-\frac{\Theta_\alpha}{3T}\right) \quad (\alpha = sh, SA, AS), \quad (11)$$

while in the case of scattering at point defects

$$\frac{1}{\tau_{imp}(\omega_n^\alpha)} = A(\omega_n^\alpha)^4. \quad (12)$$

Here, k_B and \hbar are the Boltzmann and Planck constants, respectively; γ_α is the Grüneisen parameter, Θ_α is the Debye temperature and v_α is the velocity of phonons of α -polarization; V_0 and M are the atomic volume and the average mass per one atom in the crystal, respectively [28].

According to the Matthiessen's rule, the complete relaxation time is determined by the relationship

$$\frac{1}{\tau_c} = \frac{1}{\tau_N} + \frac{1}{\tau_U} + \frac{1}{\tau_{imp}}. \quad (13)$$

Substituting it into equation (2), one can calculate the thermal conductivity coefficient κ_L . The values of the necessary parameters γ_α and Θ_α are estimated by a following way.

The intensity of scattering by impurity ions A is determined by their concentration. Its value estimated for Si crystals is $0.132 \cdot 10^{-44} \text{ s}^3$ [28, 31] and similar one: $(0.11 \dots 0.31) \cdot 10^{-44} \text{ s}^3$ for GaAs [32]. The Grüneisen parameter is expressed through the thermodynamic parameters of the crystal: the volumetric coefficient of thermal expansion (α_v), the specific heat at constant pressure (c_p) and the velocity of sound in the medium (v) [33]:

$$\gamma = \alpha_v v^2 / c_p. \quad (14)$$

Accurate calculations were performed for the example of nanofilms of a layered crystal with hexagonal symmetry (2H- PbI_2 polytype) with the following physical parameters: $a = 4.55 \text{ \AA}$ is the lattice constant in the film plane and $c = 6.98 \text{ \AA}$ – in the perpendicular direction; $V_0 = \sqrt{3}a^2c/6$ is the atomic volume and $M = 153.56 \text{ a.m.u.}$ is the average mass [23].

We used the parameters α_v and c_p of magnitudes $108 \cdot 10^{-6} \text{ K}^{-1}$ [34] and $170.7 \text{ J}/(\text{kg} \cdot \text{K})$ [9], respectively, which were measured in bulk lead iodide crystals at 300 K. The propagation velocity v of the vibrations of each polarization $\alpha = \{sh, SA, AS\}$ was assumed to be equal to the average value of the group velocities \bar{v}^α of the phonons of the respective mode of the spectrum, calculated for 2H-PbI₂-type nanofilms with different thicknesses $d = N \cdot c$ and temperatures T according to the procedure described in [25]. The parameter Θ_α for each mode of the phonon spectrum is determined by the maximal frequency ω_{\max}^α of the vibration state with a quantum number n . It is taken into account at a fixed nanofilm thickness (the Debye or cutoff frequency [35]).

According to the results of these calculations (Fig. 1), a common tendency for phonons of all polarizations is decreasing values of averaged velocities at decreasing nanofilm's thickness. An increasing temperature leads to their nonlinear growth with saturation at higher than room temperatures.

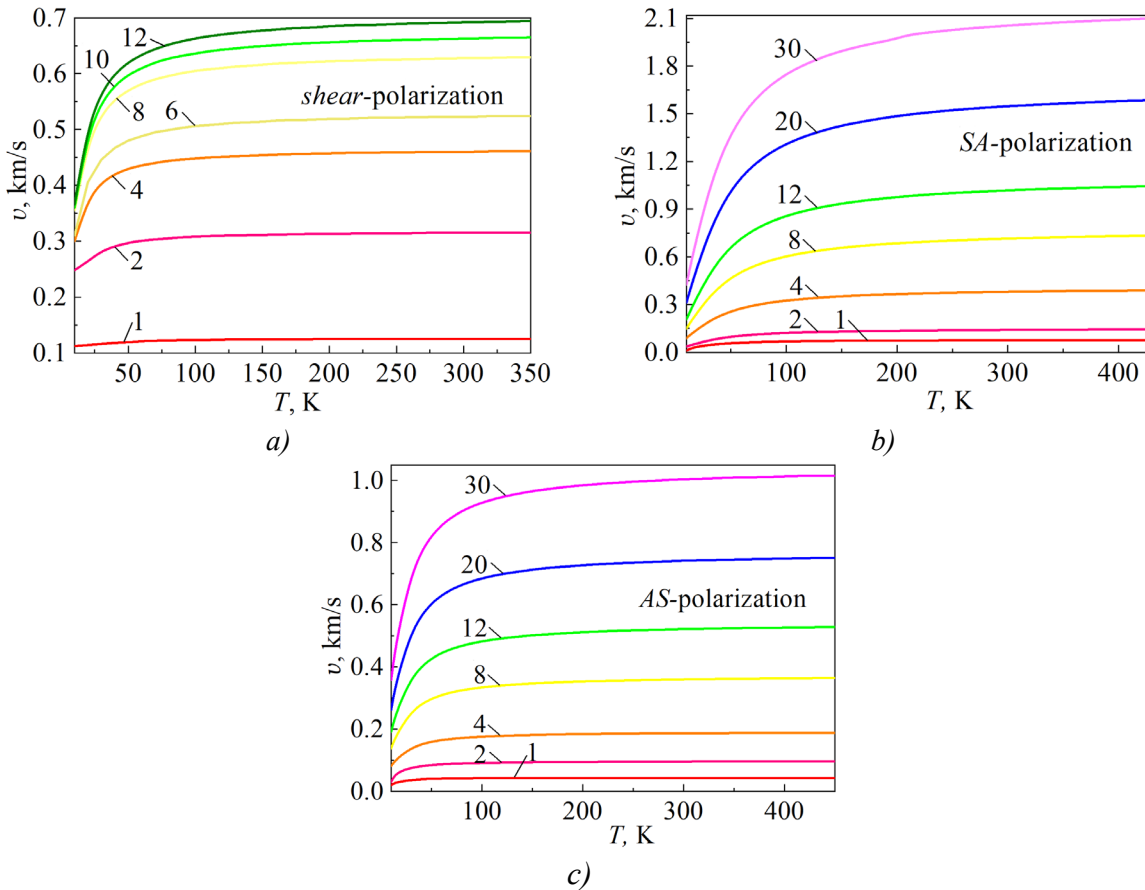


Fig. 1. Temperature dependences of the averaged propagation velocities of shear (a), dilatational (b) and flexural (c) vibrations in 2H-PbI₂ nanofilms with $d = N \cdot c$ (number N of PbI₂ layer packages is presented near the respective curve)

The results of calculations of thermal conductivity coefficient determined by the scattering of phonons of each mode of confined acoustic vibrations in lead iodide nanofilms, performed within the framework of the selected approximations, are shown in Fig. 2.

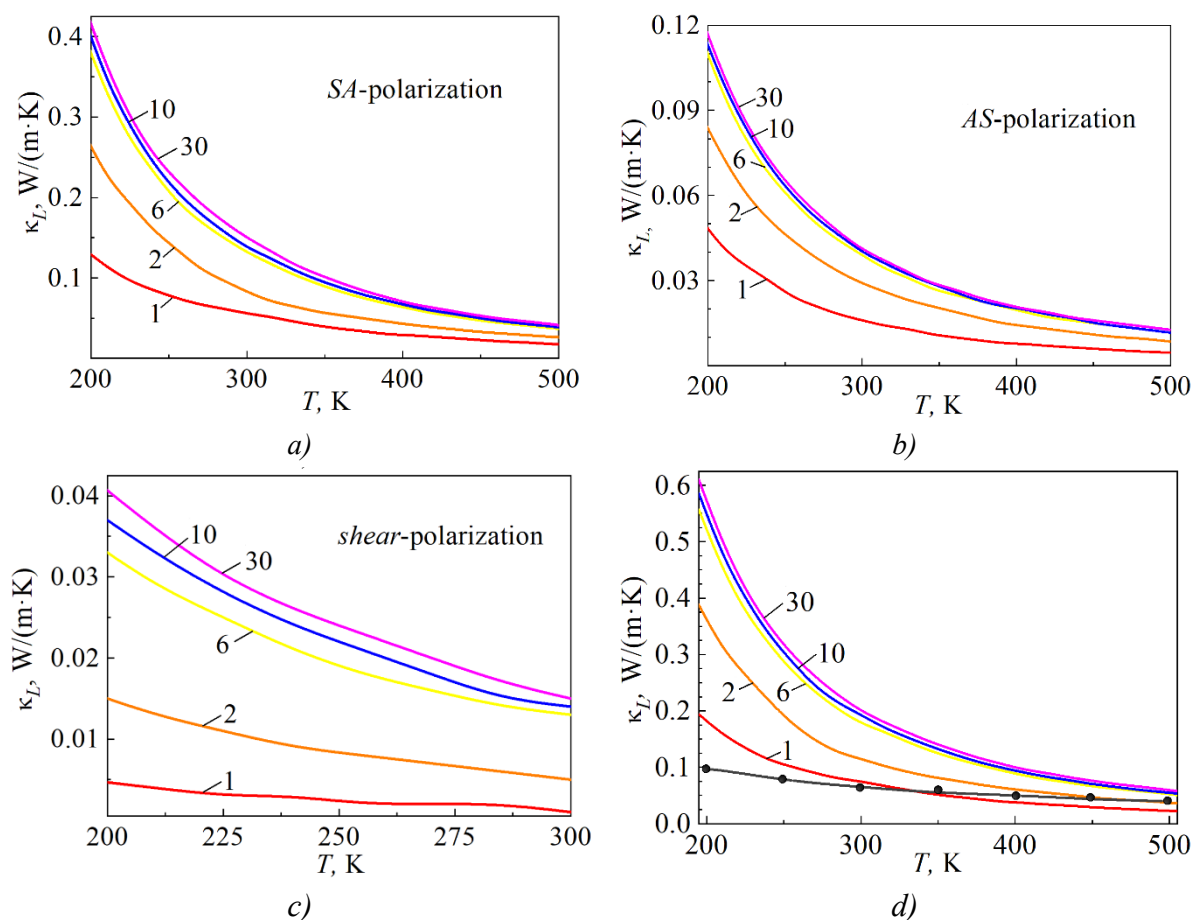


Fig. 2. Temperature dependences of the partial components (a, b, c) and complete value of thermal conductivity coefficient of the crystal lattice (d) of 2H-PbI₂ nanofilms with different thicknesses (indicated by the number N of PbI₂ layer packages).
The curve —●— is constructed according to the data of ref. [16]

Finally, using the magnitudes of S and σ , calculated in [16] for monolayer lead iodide at different temperatures, setting $L = 2.5 \cdot 10^{-8} \text{ V}^2/\text{K}^2$ and using the temperature dependences of the thermal conductivity coefficient presented here, we can estimate the value of the thermodynamic figure of merit (1). The obtained magnitudes of ZT in the case of 2H-PbI₂ nanofilms ($N = 1$) doped by donor and acceptor impurities with concentration $1.9 \cdot 10^{12} \text{ cm}^{-2}$ are shown in Table 1.

Table 1

Estimated thermodynamic figure of merit ZT of a monolayer lead iodide nanofilm with electron (ZT_e) and hole (ZT_h) type of conductivity

ZT		300 K	345 K	400 K	500 K
ZT_e	our calculations	0.6	1.33	2.07	3.54
	data [16]	1	1.33	1.67	2.33
ZT_h	our calculations	0.32	0.47	0.35	0.3
	data [16]	0.4	0.47	0.33	0.23

3. Discussion and conclusions

The analysis of the results shows the following.

1. For all types of vibrations, in the temperature region above 200 K, the contribution of phonon relaxation due to Umklapp processes is dominant. The contribution of the normal phonon-phonon scattering mechanism does not exceed 0.5 % of the Umklapp process one at arbitrary nanofilm thickness and temperature. Scattering at ionized impurities for the parameter $A = 2 \cdot 10^{-44} \text{ s}^3$, corresponding to the moderate degree of doping, increases the partial components κ_L^a of the thermal conductivity coefficient by 2...30 %, depending on the nanofilm thickness and phonon polarization.
2. The largest contribution to the lattice thermal conductivity coefficient (2) is demonstrated by the scattering of SA-polarization phonons (Fig. 2, *a*). The magnitudes of the partial components κ_L^{AS} (Fig. 2, *b*) and κ_L^{sh} (Fig. 2, *c*) are 2.6...3.8 and 10...27.5 times smaller, respectively, depending on the thickness and temperature of the nanofilm.
3. The decreasing values of propagation velocity of acoustic phonons and nanofilm thickness lead to the smaller values of the partial components (Fig. 2, *a-c*) and the complete value of the lattice thermal conductivity coefficient (Fig. 2, *d*).
4. If the temperature increases from 200 to 500 K, the lattice thermal conductivity of 2H-PbI₂ nanofilms decreases rapidly according to a nonlinear law (Fig. 2, *d*). For the ultrathin nanofilms (containing less than 6 layers), thermal conductivity is approximately four times smaller, while for the thicker layers ($N > 6$), the decreasing becomes even more essential (by a factor of six). At temperatures above 500 K, this coefficient, as well as the phonon propagation velocities, almost do not change. These results are consistent with the data of other authors. According to the results of theoretical calculations [16], the thermal conductivity of the crystal lattice of monolayer 2H-PbI₂ in this range decreases from 0.096 to 0.04 W/(m·K) (see Fig. 2, *d*). Its magnitude calculated by the authors of ref. [23] is 0.052 W/(m·K) at room temperatures. The discrepancies between our results and those presented in the cited papers are explained by the use of different sets of calculation parameters, models, and methods within which they were obtained. We should also note that, according to the experimental measurements [19], the thermal conductivity coefficient of bulk lead iodide exceeds the values presented here for the nanofilms based on it. For the direction corresponding to the planes of the layer packets, its value is 0.681 W/(m·K) at 300 K and also rapidly decreases to 0.391 W/(m·K) at 497.5 K.
5. The estimation of the thermoelectric figure of merit ZT , performed for the example of a 2H-PbI₂ monolayer nanofilm, correlates with the data of ref. [16] and confirms their prediction of the perspectives for using quasi-2D structures based on lead iodide to fabricate thermoelectric devices, which can operate in the range of room and higher temperatures. The thermal conductivity coefficient of the crystal lattice of nanofilms, formed from two or more 2H-PbI₂ layer packages, approaches the value obtained for the case of a monolayer film (Fig. 2, *d*) at temperatures above 400 K. This gives reason to hope that they can be used as thermoelectric materials. The temperature range and figure of merit magnitude will

obviously differ for nanofilms with different thickness due to the dependence of the parameters that determine the thermal conductivity coefficient. Quantitative evaluation of these parameters requires reliably established magnitudes of these parameters and is currently unavailable.

Authors' information

- Yu.V. Lutsiuk – lecturer at the College of Yuriy Fedkovych Chernivtsi National University.
- V.M. Kramar – Doctor of Physical and Mathematical Sciences, Professor at the Department of Professional and Technology Education and General Physics.
- I.A. Konstantynovych – Candidate of Physical and Mathematical Sciences, Associated Professor (Docent) at the Department of Thermoelectricity and Medical Physics.
- O.M. Voitsekhivska – Candidate of Physical and Mathematical Sciences, Associated Professor (Docent) at the Department of Information Technologies and Computer Physics.

References

1. Anatyshchuk L.I., Vikhor L.N. (2012). *Thermoelectricity: Monohraf. Vol. IV. Functionally graded thermoelectric materials*. Institute of Thermoelectricity, Kyiv, Chernivtsi. 180 p. ISBN 978-966-399-410-9.
2. Tsakalakos T. (2003). Nanostructures and Nanotechnology: Perspectives and New Trends. *Nanostructures: Synthesis, Functional Properties and Applications. NATO Science Series / T. Tsakalakos, I.A. Ovid'ko, A.K. Vasudevan (Eds). Series II: Mathematics, Physics and Chemistry, Vol. 128*. Springer, Dordrecht.
https://link.springer.com/chapter/10.1007/978-94-007-1019-1_1
3. Venkatasubramanian R., Siivola E., Colpitts Th. & O'Quinn B. (2011). Thin-film thermoelectric devices with high room-temperature figures of merit. *Nature* 413, 597–602. doi:10.1038/35098012.
4. Pennelli D. (2014). Review of nanostructured devices for thermoelectric applications. *Beilstein J. Nanotechnol.* 5, 1268–1284. doi:10.3762/bjnano.5.141
5. Tayari V., Senkovskiy B.V., Rybkovskiy D., et. al. (2018). Quasi-two-dimensional thermoelectricity in SnSe. *Phys. Rev. B* 97, 045424.
<https://doi.org/10.1103/PhysRevB.97.045424>
6. Liu X., Ha S.T., Zhang Q., et al. (2015). Whispering Gallery Mode Lasing from Hexagonal Shaped Layered Lead Iodide Crystals. *ACS Nano* 9(1), 687–695.
<https://doi.org/10.1021/mn5061207>
7. Lu N., Guan J. (2022). Thermoelectric performance of XI_2 ($X = Ge, Sn, Pb$) bilayers. *Chinese Phys. B* 31, 047201. DOI 10.1088/1674-1056/ac474C
8. Hu Y.F., Yang J., Yuan Y.Q., & Wang J.W. (2019). GeI_2 monolayer: a model thermoelectric material from 300 to 600 K. *Phil. Magazine* 100(6), 782–796.
<https://doi.org/10.1080/14786435.2019.1699670>

9. Naseri M., Hoat D.M., Salehi K., Amirian S. (2020). Theoretical prediction of 2D XI_2 ($X = Si, Ge, Sn, Pb$) monolayers by density functional theory. *J. Mol. Graph. Model.* 95, 107501. <https://doi.org/10.1016/j.jmglm.2019.107501>
10. Zhong M., Zhang S., Huang L., et al. (2017). Large-scale 2D PbI_2 monolayers: experimental realization and their band-gap related properties. *Nanoscale* 9(11), 3736–3741. DOI:10.1039/C6NR07924E
11. Zheng W., Zhang Z., Lin R., et al. (2016). High-crystalline 2D layered PbI_2 with ultrasmooth surface: liquid-phase synthesis and application of high-speed photon detection. *Adv. Electron. Mater.* 2(11), 1600291. DOI:10.1002/aelm.201600291
12. Wangyang P., Sun H., Zhu X., et al. (2016). Mechanical exfoliation and Raman spectra of ultrathin PbI_2 single crystal. *Mater. Lett.* 168, 68–71. DOI:10.1016/j.matlet.2016.01.034
13. He K., Zhu J., Li Z. et al. High-sensitive two-dimensional PbI_2 photodetector with ultrashort channel. *Front. Phys.* 18, 63305 (2023) (Special Topic: Two-dimensional Electronic Materials and Devices ISSN: 2095–0462 (Print) 2095–0470 (Online)). <https://doi.org/10.1007/s11467-023-1323-1>
14. K.S. Shah, F. Olschner, L.P. Moy, et al. (1996). Lead iodide X-ray detection systems. *Nuclear Instruments and Methods in Physics Research Section A: Accelerators, Spectrometers, Detectors and Associated Equipment.* 380(1–2), 266–270. ISSN 0168-9002, [https://doi.org/10.1016/S0168-9002\(96\)00346-4](https://doi.org/10.1016/S0168-9002(96)00346-4).
15. K.S. Shah, P. Bennett, M. Klugerman, et al. (1997). Lead iodide optical detectors for gamma ray spectroscopy. *IEEE Transactions on Nuclear Science* 44(3), 448–450. doi: 10.1109/23.603688.
16. Peng B., Mei H., Shao H., et al. (2019). High thermoelectric efficiency in monolayer PbI_2 from 300 K to 900 K. *ArXiv: 1811.04244v2 [cond-mat.mtrl-sci]*. <https://www.osti.gov/servlets/purl/1556115>
17. Zincenco N.D., Nika D.L., Pokatilov E.P., and Balandin A.A. (2007). Acoustic phonon engineering of thermal properties of silicon-based nanostructures. *J. Phys.: Conf. Ser.* 92, 012086. DOI: 10.1088/1742-6596/92/1/012086
18. Balandin A.A., Pokatilov E.P., Nika D.L. (2007). Phonon engineering in hetero- and nanostructures. *J. Nanoelectron. Optoelectron.* 2, 140–170. <https://doi.org/10.1166/jno.2007.201>
19. Cröll A., Tonn J., Post E., et al. (2017). Anisotropic and temperature-dependent thermal conductivity of PbI_2 . *J. Cryst. Growth*, 466, 16–21. <http://dx.doi.org/10.1016/j.jcrysgro.2017.03.006>
20. Ran R., Cheng C., Zeng Z., et al. (2019). Mechanical and thermal transport properties of monolayer PbI_2 via first-principles investigations. *Phil. Magazine*, 99(10), 1277–1296. <https://doi.org/10.1080/14786435.2019.1580818>
21. Guo P., Stoumpos C.C., Mao L. et al. (2018). Cross-plane coherent acoustic phonons in two-dimensional organic-inorganic hybrid perovskites. *Nat. Commun* 9, 2019. DOI: 10.1038/s41467-018-04429-9

22. Yağmurcukardeş M., Peeters F.M., Sahin H. (2018). Electronic and vibrational properties of PbI₂: from bulk to monolayer. *Phys. Rev. B* 98, 085431.
DOI: 10.48550/arXiv.1807.09140
23. Bolen E., Deligoz E., Ozisik H. (2021). Origin of low thermal conductivity in monolayer PbI₂. *Solid State Communications* 327, 114223. <https://doi.org/10.1016/j.ssc.2021.114223>
24. Lutsiuk Yu., Kramar V., Petryk I. Frequency spectrum and group velocities of acoustic phonons in PbI₂ nanofilms. *Phys. Chem, Solid St.* 23(3), 478–483.
<https://doi.org/10.15330/pcss.23.3.478-483>
25. Lutsiuk Yu. (2024). Temperaturni zalezhnosti userednennykh hrupovykh shvydkostey akustychnykh fononiv u ploskykh nanoplivkakh dyodydu svyntsyu [Temperature dependences of the averaged group velocities of acoustic phonons in flat nanofilms of lead iodide]. *Physics and Educational Technology*, 2, 40–46.
<https://doi.org/10.32782/pet-2024-2-6>
26. Bannov N., Mitin V., Stroschio M. (1994). Confined acoustic phonons in a free-standing quantum well and their interaction with electrons. *Phys. Stat. Sol.(b)* 183(1), 131–142.
<https://doi.org/10.1002/pssb.2221830109>
27. Pokatilov E.P., Nika D.L., Balandin A.A. (2003). Phonon spectrum and group velocities in AlN/GaN/AlN and related heterostructures. *Superlattices and Nanostructures* 33, 155–171.
[https://doi.org/10.1016/S0749-6036\(03\)00069-7](https://doi.org/10.1016/S0749-6036(03)00069-7)
28. Zhang Y. (2016). First-principles Debye-Callaway approach to lattice thermal conductivity. *J. Materiomics* 2, 237–247. <https://doi.org/10.1016/j.jmat.2016.06.004>
29. Lutsiuk Yu.V., Kramar V.M. (2020). Analytical Calculation of Frequency Spectrum and Group Velocities of Acoustic Phonons in Quasi-two-dimensional Nanostructures. *J. Nano-Electron. Phys.* 12(5), 05033. [https://doi.org/10.21272/jnep.12\(5\).05033](https://doi.org/10.21272/jnep.12(5).05033)
30. Street R.A., Mulato M., Schieber M. et al. (2001). Comparative study of PbI₂ and HgI₂ as direct detector materials for high resolution X-ray image. *Proc. SPIE* 4320, 1–12.
DOI:10.1117/12.430858
31. Holland M.G. Analysis of lattice thermal conductivity. *Phys. Rev.*132, 2461. DOI: <https://doi.org/10.1103/PhysRev.132.2461>
32. Ansari M., Ashokan V., Indu B., Kumar R. (2012). Lattice thermal conductivity of GaAs. *Acta Phys. Polonica A* 121(3), 639–646. DOI:10.12693/APhysPolA.121.639
33. Grüneisen E. (1912). Theorie des festen Zustandes einatomiger Elemente. *Annalen der Physik* 344(12), 257–306. DOI: 10.1002/andp.19123441202
34. Nitsch K., Rodová M. (2002). Thermomechanical measurements of lead halide single crystals. *Phys. stat. solidi (b)* 234(2), 701–709.
DOI:10.1002/1521-3951(200211)234:2<701::AID-PSSB701>3.0.CO;2-1
35. Mingo N. (2003). Calculation of Si nanowire thermal conductivity using complete phonon dispersion relations. *Phys. Rev. B* 68(11), 113308.
DOI: <https://doi.org/10.1103/PhysRevB.68.113308>

Submitted: 22.05.2025

Луцюк Ю.В.¹ (<https://orcid.org/0000-0003-1776-6734>),
Крамар В.М.^{1,2} (<https://orcid.org/0000-0002-3185-4338>),
Константинович І.А.^{1,2} (<https://orcid.org/0000-0001-6254-6904>),
Войцехівська О.М.¹ (<https://orcid.org/0000-0003-2118-231X>)

¹Чернівецький національний університет імені Юрія Федьковича,
вул. Коцюбинського 2, Чернівці, 58012, Україна;

²Інститут термоелектрики НАН та МОН України,
вул. Науки, 1, Чернівці, 58029, Україна

Вплив акустичних фононів на термоелектричні властивості наноплівки дийодиду свинцю

У наближенні пружного континууму методами теорії пружності досліджено вплив просторових обмежень на швидкості поширення акустичних фононів у плоских квазідвовимірних наноструктурах (наноплівках) на основі шаруватого напівпровідника $2H-PbI_2$, величину коефіцієнта теплопровідності та термоелектричну добротність таких структур. Показано, що найбільший вплив на величину коефіцієнта теплопровідності наноплівки дийодиду свинцю справляють акустичні фонони, що належать гілці дилатаційних коливань атомів кристалічної ґратки. Переважним механізмом релаксації усіх типів обмежених акустичних фононів у наноплівці за умови помірної концентрації домішок в ній є фонон-фононна (Umklapp) взаємодія, ефективність якої щодо розсіювання залежить від товщини наноплівки та її температури. Від цих параметрів також залежить швидкість поширення фононів. Указані фактори спричиняють стрімке зменшення коефіцієнта теплопровідності наноплівки із зменшенням її товщини і збільшенням температури, що сприяє збільшенню термодинамічної добротності наноструктури. Оцінка величини термодинамічної добротності ультратонких (у декілька шарових пакетів $2H-PbI_2$) плівок дозволяє зробити висновок про їх придатність для створення термоелектричних пристроїв, здатних працювати в області кімнатних температур і вище.

Ключові слова: наноструктура, наноплівка, фонон, спектр частот і групових швидкостей, теплопровідність, термоелектрична добротність, термоелектричні матеріали, дийодид свинцю.

Надійшла до редакції 22.05.2025